Climate
of the Past

Expression of the "4.2 ka event" in the southern Rocky Mountains, USA

David T. Liefert and Bryan N. Shuman

Department of Geology and Geophysics, University of Wyoming, Laramie, WY 82071, USA

Correspondence: David T. Liefert (dliefert@openspace.org)

Abstract. The use of the climatic anomaly known as the "4.2 ka event" as the stratigraphic division between the middle and late Holocene has prompted debate over its impact, geographic pattern, and significance. The anomaly has primarily been described as abrupt drying in the Northern Hemisphere at ca. 4 ka (ka, thousands of years before present), but evidence of the hydroclimate change is inconsistent among sites both globally and within North America. Climate records from the southern Rocky Mountains demonstrate the challenge with diagnosing the extent and severity of the anomaly. Dune-field chronologies and a pollen record in southeastern Wyoming reveal several centuries of low moisture at around 4.2 ka, and prominent low stands in lakes in Colorado suggest the drought was unique amid Holocene variability, but detailed carbonate oxygen isotope ($\delta^{18}O_{carb}$) records from Colorado do not record drought at the same time. We find new evidence from $\delta^{18}O_{carb}$ in a small mountain lake in southeastern Wyoming of an abrupt reduction in effective moisture or snowpack from approximately 4.2–4 ka, which coincides in time with the other evidence of regional drying from the southern Rocky Mountains and the western Great Plains. We find that the $\delta^{18}O_{carb}$ in our record may reflect cool-season inputs into the lake, which do not appear to track the strong enrichment of heavy oxygen by evaporation during summer months today. The modern relationship differs from some widely applied conceptual models of lake–isotope systems and may indicate reduced winter precipitation rather than enhanced evaporation at ca. 4.2 ka. Inconsistencies among the North American records, particularly in $\delta^{18}O_{carb}$ trends, thus show that site-specific factors can prevent identification of the patterns of multi-century drought. However, the prominence of the drought at ca. 4 ka among a growing number of sites in the North American interior suggests it was a regionally substantial climate event amid other Holocene variability.

1 Introduction

Rapid climate changes are well documented in the late Pleistocene and early Holocene, such as during the Younger Dryas chronozone (ca. 12.9–11.7 ka, thousands of years before present) and at 8.2 ka (Alley et al., 1997; Clark et al., 1999; Von Grafenstein et al., 1998), but middle to late Holocene changes are less well understood (Wanner et al., 2008, 2011). One potential abrupt change during this time, a multi-century climatic anomaly known as the "4.2 ka event," has been used as the benchmark for the stratigraphic division between the middle and late Holocene (Walker et al., 2019). Consequently, the 4.2 ka event has become a topic of scrutiny with debate over its impact, geographic pattern, and significance (Bradley and Bakke, 2019; Weiss, 2016, 2019). The ostensibly global event has primarily been described as a dry episode at low and midlatitudes (Booth et al., 2005; Nakamura et al., 2016; Di Rita and Magri, 2019; Scuderi et al., 2019; Xiao et al., 2018). However, some regions show increased precipitation (Huang et al., 2011; Railsback et al., 2018) or no change (Roland et al., 2014), as is consistent with spatial variation expected from climate variability that shifts atmospheric waves and dynamics.

The 4.2 ka event has been widely examined, but its cause and significance amid other millennial-to-centennial climate variability during the Holocene remain unknown. Processes that may have been involved in the event included changes in solar irradiance (Wang et al., 2005), centennial-scale atmospheric circulations (Deininger et al., 2017), and latitudi-

nal shifts in the Intertropical Convergence Zone (Tan et al., 2008). Recent model simulations have produced similar patterns of extended drought in the Northern Hemisphere without external forcings such as insolation changes or volcanism (Yan and Liu, 2019), and others confirm that multi-decadal megadroughts can arise through internal climate variability without changes in boundary conditions (Ault et al., 2018). Internal climate dynamics and feedbacks could also interact with stochastic variability and external forcing to produce such events without consistent or linear relationships to the forcing; forcing may only have a modest probability of triggering rapid climate changes (Renssen et al., 2006). Less clear is how unusual or frequent prolonged "megadroughts" may be within the Holocene across different regions.

That such droughts can occur stochastically indicates the 4.2 ka event could be an example of typical late Holocene climate variability at multi-century timescales (Shuman and Burrell, 2017), even if the event was exceptional within the spectrum of Holocene variability in some regions. For example, the event is recorded in the northeastern United States as one drought period within a series of Holocene wetting and drying events (Newby et al., 2014; Shuman et al., 2019; Shuman and Burrell, 2017); evidence for a major hydroclimate change at ca. 4 ka has been growing in the North American mid-continent (Booth et al., 2005; Carter et al., 2018; Dean, 1997; Denniston et al., 1992; Halfen and Johnson, 2013; Jiménez-Moreno et al., 2019). However, the event's significance or uniqueness has been difficult to verify in this region because few sites document the anomaly compared to other regions of the midlatitudes globally (Ran and Chen, 2019; Zhang et al., 2018).

Records from the southern Rocky Mountains of North America demonstrate the challenge. In the midlatitude Rocky Mountains, only dune-field chronology and pollen records have been explicitly interpreted to show the 4.2 ka event, while other record types, such as stable isotopes, have not. Initial recognition in North America derived from the timing of the reactivation of the Ferris, Seminoe, and Casper dune fields in southeastern Wyoming (Fig. 1, Table 1; Booth et al., 2005; Halfen et al., 2010; Stokes and Gaylord, 1993), but the extent of the drought has been unclear because other dune-field chronologies in the adjacent western Great Plains do not clearly document the drought (Dean, 1997; Halfen and Johnson, 2013; Mason et al., 1997). More recently, Carter et al. (2013, 2017, 2018) used fossil pollen from Long Lake in the Medicine Bow Mountains, south of the Wyoming dune fields (Fig. 1, Table 1), to identify a 150-year interval of increased temperature and decreased precipitation centered at 4.2 ka. The inferred precipitation reductions were largest in springtime (Carter et al., 2018), when snowfall in the southern Rocky Mountains is highest today (Mock, 1996). Consistent with this interpretation, stratigraphic evidence of lake-level changes in Colorado and Wyoming lakes could indicate that low-water phases at ca. 4.2 ka were one of the most prominent hydrologic changes during the Holocene

(Jiménez-Moreno et al., 2019; Shuman et al., 2009, 2014, 2015). The drying event stands out as one of the only multi-centennial features in a summary of low lakes in the Rocky Mountains during the late Quaternary (Shuman and Serravezza, 2017).

By contrast, the 4.2 ka event does not appear in stable oxygen isotope records from lakes in the same region, such as detailed carbonate $\delta^{18}O$ ($\delta^{18}O_{carb}$) records from Bison and Yellow lakes, Colorado (Fig. 1, Table 1; Anderson, 2011, 2012). Widely applied conceptual models of lake–isotope systems indicate that climate-driven changes in the stable isotope composition of lake water become archived in lacustrine carbonates (e.g., Anderson et al., 2016; Leng and Marshall, 2004; Talbot, 1990). According to such models, site-specific hydrologic controls on isotope budgets and the timing of carbonate formation should also play an important role in how the 4.2 ka event was recorded, but the isotopic response should vary predictably by hydrologic setting: long lake-water residence times and high evaporation cause hydrologically closed lakes (i.e., terminal basins) to record shifts in effective moisture (precipitation–evaporation) because endogenic carbonates typically precipitate in evaporated, ^{18}O-rich water during the warm summer months. Drought could drive a positive change in the isotope composition of lake water within such a lake–isotope system by both increasing evaporation and changing seasonal precipitation, such as by reducing snowpack. In hydrologically open lakes with short residence times, the continual replacement of evaporated water creates isotopic sensitivity, primarily to the seasonal balance of precipitation, without a strong evaporation effect. In either model, $\delta^{18}O_{carb}$ tracks the isotope composition of lake water and its response to climate changes.

Many lakes fall somewhere between fully hydrologically open and closed, and additional site-specific influences may also override such expectations. Consequently, not all stable oxygen isotope records from lakes may have been sensitive to the specific climate variables that changed at 4.2 ka. Modern lake-water isotopic measurements (Fig. 2) can help to identify the relative influences of different controls on the magnitude and range of lake-water $\delta^{18}O$, such as groundwater fluxes and other seasonal dynamics that modify lake-water residence times. We examine how the seasonality of carbonate formation could cause the relationships of lake-water $\delta^{18}O$ to $^{18}O_{carb}$ to differ from the modern patterns observable in lakes today.

Here we present a new $\delta^{18}O_{carb}$ record from Highway 130 Lake (HL) in southeastern Wyoming near where other Holocene paleohydrological and paleoecological records have been developed (Fig. 1, Table 1; Mensing et al., 2012; Minckley et al., 2012; Brunelle et al., 2013). HL is an intermittently closed subalpine lake in the Medicine Bow Mountains within 20 km of Long Lake, where fossil pollen indicates a prolonged "megadrought" at 4.2 ka (Carter et al., 2018). The lake is also < 60 km from Upper Big Creek Lake, Colorado, where a prominent paleoshoreline detected in geo-

physical surveys and cores indicates low water after 4.7 ka (Fig. 1, Table 1; Shuman et al., 2015). Previous work at HL indicates a strong influence of evaporation on the lake and the stable isotope composition of its water, which we compare with Bison and Yellow lakes in Colorado (Fig. 2; Liefert et al., 2018). We discuss how dissimilarities in $\delta^{18}O_{carb}$ among lakes, possibly driven by non-climatic factors, could complicate interpretations of the patterns of past hydroclimate changes including megadroughts and Holocene trends. Together these outcomes may clarify the timescales on which drought operates within a critical headwater area of North America, but also confirm that interpretations of past hydroclimate changes using $\delta^{18}O_{carb}$ may depend heavily on site-specific dynamics.

2 Site description

HL (41°21′05″ N, 106°15′50″ W; 3199 m a.s.l., above sea level) fills a shallow depression in the uneven terrain covering the Libby Creek watershed (12 km² surface area) in the Snowy Range, a southwest-trending subsection of the Medicine Bow Mountains in southeastern Wyoming (Fig. 1). Around HL, subalpine coniferous forests interspersed with open meadows grow on thin glaciated soils and tills between the frequent outcroppings of the underlying siliceous metadolomite (Houston and Karlstrom, 1992; Musselman et al., 1992). Southeastern Wyoming has a semi-arid climate, but the Medicine Bow Mountains receive about 1000 mm of precipitation each year, with approximately 70 % of annual totals falling as snow from October to June (Mock, 1996). Local average wind speeds are high ($\sim 5 \, \mathrm{m \, s^{-1}}$), and minimum winter and maximum summer temperatures typically reach −23 and 21 °C, respectively (SNOTEL station ID 367).

The surface watershed around HL occupies $\sim 0.45 \, \mathrm{km^2}$, while the lake has a surface area of $\sim 0.02 \, \mathrm{km^2}$, a maximum (spring) water depth of $\sim 200 \, \mathrm{cm}$, and declines in water level by $\sim 30 \, \mathrm{cm}$ from July to late October (Liefert et al., 2018). Ice covers HL from approximately October to May, and stream connections shut off in June following spring flooding. Measurements reveal no thermal stratification because of the shallow water depth, flat-bottom bathymetry, and high average wind speeds, which promote mixing throughout the water column (Bello and Smith, 1990; Stewart and Rouse, 1976). Liefert et al. (2018) found that evaporation could account for as much as 83 % of the seasonal water loss at HL, though the stable water level and temperature compared to nearby lakes of similar size and depth indicate shallow groundwater flow-through driven by seasonal precipitation and infiltration (Rautio and Korkka-Niemi, 2011; Rosenberry and LaBaugh, 2008).

3 Methods

To measure the modern oxygen and hydrogen isotope compositions of the lake water ($\delta^{18}O$ and δD, respectively), temperature, and specific conductance, water samples were collected at approximately biweekly intervals from June to October in each year from 2015–2017. Additional samples of snowfall, snowpack, rain, and groundwater (from springs and wells) were collected episodically from 2015–2017 to measure the range in water isotope values of the watershed's hydrologic components. Isotopic ratios of all water samples were measured at the University of Wyoming Stable Isotope Facility using a Picarro L2130-I cavity ring-down spectrometer, and specific conductance was measured using a YSI multiparameter water quality meter. We report $\delta^{18}O$ and δD in the per mill (‰) notation relative to Vienna Standard Mean Ocean Water (VSMOW). We acquired meteorological data from SNOTEL stations near HL at Brooklyn Lake, Wyoming (ID 367; 3121 m a.s.l.; 41.36° N, −106.23° W), and at Bison Lake, Colorado (ID 345; 3316 m a.s.l.; 39.76° N, −107.36° W), to compare the modern ratios of snow to rain that control the seasonal balance of precipitation at the lakes.

In October 2016 we installed a pressure transducer (Onset HOBO U20 level data logger) to measure the water level and temperature of HL at 30 min intervals; freezing conditions required that we secure the transducer to the lake bed inside a bladder filled with antifreeze. To compensate for barometric pressure changes we adjusted the transducer data using pressure measurements from the nearby Glacier Lakes Ecosystem Experiments Site Brooklyn Tower AmeriFlux site (GLEES Tower; US-GLE: https://ameriflux.lbl.gov/sites/siteinfo/US-GLE, last access: January 2019; 41°21′57″ N, 106°14′23″ W; 3191 m a.s.l.). In late January 2017, we installed a conductivity data logger (Onset HOBO U24 conductivity data logger) at the same location and water depth as the pressure transducer to measure the range in conductivity (converted to specific conductance at 25 °C) at 30 min intervals of the unfrozen water underlying the ice cover to examine the seasonal patterns of water chemistry that influence carbonate formation.

On the same day in January 2017, we collected a 70 mm diameter sediment core with a modified Livingston piston corer from the center of HL where the combined water and ice depth reached approximately 90 cm; we used this depth to calibrate the pressure transducer. The organic and carbonate content of contiguous 1 cm intervals of the sediment core were measured by weighing the residual sediment after burning the samples at 550 and 1000 °C, respectively. After the 550 °C burn removed organic matter, we isolated 1 cm³ subsamples from each interval for isotopic analysis; $\delta^{18}O_{carb}$ of samples burned was within the range of instrument uncertainty (±0.2 ‰) as those with organic removal using oxidizing agents (typically bleach), indicating no additional fractionation. Each subsample was sieved using a 63 μm mesh to
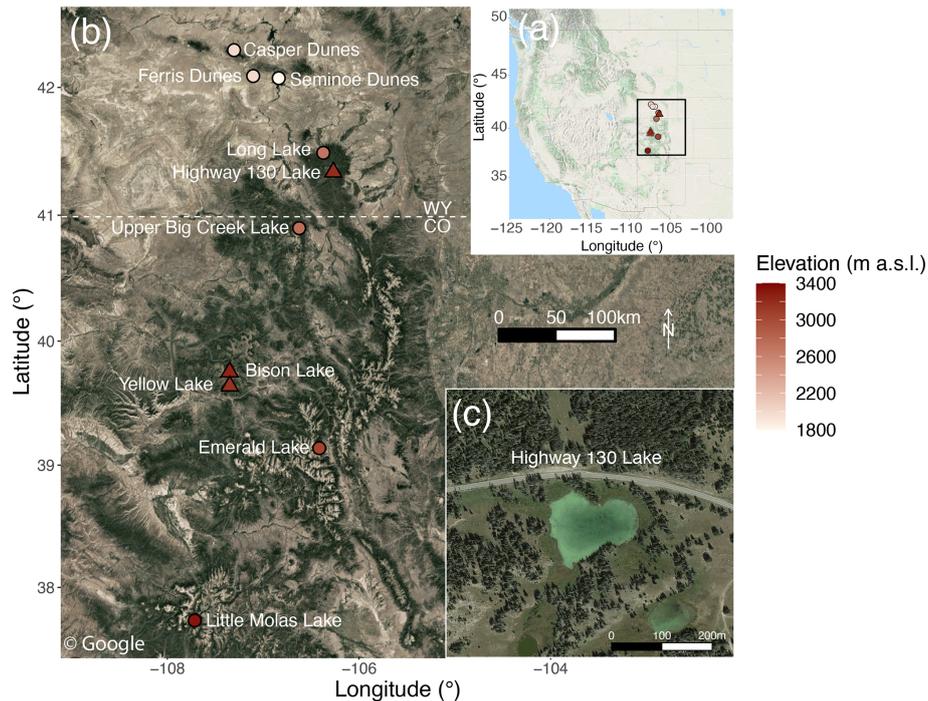
Figure 1. Locations of the study site and related climate records. **(a)** Highway 130 Lake (triangle; this study) and related carbonate (triangles), dune-field chronology, pollen, and lake-level records (circles) lie within the southern Rocky Mountains, a critical headwater area in the western United States that contributes snowmelt to the Colorado and North Platte rivers. **(b)** Study site locations in the Colorado Front Range and Medicine Bow Mountains, southeastern Wyoming. **(c)** Highway 130 Lake lies within the Snowy Range, a subsection of the Medicine Bow Mountains. Google images (© Google Maps 2021) were acquired using the ggmap package in R (Kahle and Wickham, 2013).

isolate the fine fraction to be used for isotopic analysis using a Thermo Gasbench coupled to a Thermo Delta Plus XL isotope ratio mass spectrometer at the University of Wyoming Stable Isotope Facility. X-ray powder diffraction (XRD) confirmed that the samples contained only microcrystalline calcite. We assume the calcite is predominantly autochthonous because the underlying metadolomite likely provides the Ca ions needed for carbonate formation (if the lacustrine carbonates were clastic deposits from metadolomite then its erosion should deposit more dolomite than calcite), and evidence of biogenic calcite within the core is rare (ostracod tests were present in fewer than 10 of the 300 samples). We report $\delta^{18}O_{carb}$ in the per mill (‰) notation relative to the Vienna Pee Dee Belemnite (VPDB) standard. To calculate the temperature-dependent fractionation for calcite formation and convert from VSMOW to VPDB, we use equations from Leng and Marshall (2004).

We isolated sedimentary charcoal ($> 125 \mu m$) from the sediment core for radiocarbon analyses to estimate sedimentation rates. Radiocarbon samples were analyzed at the University of California Irvine Keck Carbon Cycle facility. We calibrated the radiocarbon chronology to calendar years using intcal13 (Reimer et al., 2013) and generated the age–depth model and uncertainties using Bchron (Parnell et al., 2008) and geoChronR (McKay et al., 2021).

4   Results

4.1   Modern water chemistry and level measurements

Lake-water $\delta^{18}O$ and δD in HL increased during the ice-free season from -17.8‰ and -132‰ (sampled in late June) to -10.8‰ and -94.2‰ (sampled in late October), respectively (black circles, Fig. 2). The slope of the line tracing the seasonal range in HL's lake-water isotopes (thick black line, Fig. 2) traces the local evaporation line (LEL) defined by samples from lakes in the Colorado Front Range (red dashed line, Fig. 2; Henderson and Shuman, 2009). Several consecutive years of measurements reveal that water isotope values at HL are consistent from year to year. The LEL's deviation from both the global meteoric water line (GMWL; Fig. 2) and isotope composition of the hydrologic inputs (open symbols, Fig. 2) indicates a strong evaporative influence. $\delta^{18}O$ and δD values at HL also indicate stronger fractionation by evaporation compared to representative warm-season isotope compositions measured at Bison and Yellow lakes from June–September around 2010 (thick purple and yellow lines, Fig. 2; Anderson, 2011, 2012), which remained closer to the composition of meteoric waters. Longer lake-water residence time and higher evaporation in HL thus appear to produce a greater range of warm-season isotope compositions compared to Bison and Yellow lakes.

The different lake-water $\delta^{18}O$ values among the lakes contrasts with their similar seasonal precipitation patterns. The modern ratio of snow to rain, which can determine the mean precipitation and lake-water $\delta^{18}O$, is comparable in the watersheds of HL and Bison Lake when averaged from 1980–2019 (inset plot, Fig. 2). Other modern differences among the lakes, which all have surface areas of $< 0.1\,km^2$, indicate that the maximum water depth of HL is several meters shallower than Bison and Yellow lakes (Anderson, 2012) and that the summer lake-water temperatures in HL typically range from 8–12 °C, which is cooler than the epilimnion at Yellow Lake (Anderson, 2012). HL is also several degrees cooler than nearby lakes also without thermal stratification (Liefert et al., 2018).

Continuous measurements of specific conductance began in early February when the combined water and ice depth reached approximately 90 cm (Fig. 3). Specific conductance increased from 700 to 1115 µS cm^{-1} by early April while the lake surface was frozen. The specific conductance fell below 500 µS cm^{-1} as the lake flooded with snowmelt in early May. Specific conductance ranged from 250–300 µS cm^{-1} after the conductivity data logger was removed in late June and before the lake froze over in the fall, and the water depth stayed between 100 and 150 cm, which was low compared to previous years (Liefert et al., 2018).

4.2 Sediment characteristics

The 333 cm core from HL extends to at least the early Holocene and contains predominantly carbonate sediment underlain by silicate clays (Fig. 4). The upper 303 cm contains 5 %–55 % organics and 5 %–90 % carbonate; the core above the basal 30 cm has a mean carbonate content of 65%. In the basal unit, the carbonate content drops below 5 %, which was too low for isotopic analysis. The age–depth model (black line with 2σ gray uncertainty band, Fig. 4, Table 2) reveals average net sediment accumulation rates of 18 cm kyr^{-1} (thousand years) from 11.7–4.4 ka and 45.5 cm kyr^{-1} from 4.4 ka to present. High rates of net sedimentation correspond to intervals of high carbonate flux into the lake, indicating that authigenic carbonate production may largely control sedimentation rates. The carbonate content and carbonate flux, representing the mass of carbonates deposited per unit area per year, increased simultaneously with the sedimentation rate at 4.4 ka (Fig. 4), but the percent carbonate content subsequently declined until 4.0 ka. The radiocarbon age at 119 cm depth (3.072 ± 0.03 ka) has an age similar to the date at 67 cm depth (3.031 ± 0.02 ka), which may indicate a reworked upper age (black dots in Fig. 4). However, high total sediment and carbonate accumulation rates are inferred even if the upper age was excluded from the age–depth model.

4.3 Sedimentary oxygen and carbon isotopes

$\delta^{13}C_{carb}$ and $\delta^{18}O_{carb}$ in the upper 303 cm of sediment range from −6.9‰ to −1.5‰ and −18.4‰ to −15.2‰, respectively, and the mean isotope compositions become more positive over the record, but there is no significant trend (Fig. 4). Variance in $\delta^{13}C_{carb}$ and $\delta^{18}O_{carb}$ is highest before 4.4 ka (below 200 cm depth) and lowest since 1.5 ka (above 40 cm depth; Fig. 5). Isotope excursions appear in both the slow and fast sedimentation intervals and when the carbonate flux is both low and high (Fig. 4). $\delta^{18}O_{carb}$ peaks (2.9 standard deviations above the mean) from approximately 4.2–4 ka, for which four calibrated radiocarbon ages constrain the timing and indicate a fast sedimentation rate (Fig. 5). The carbonate flux is high, but the carbonate content is low (~ 55 %) during this interval relative to the mean (Fig. 4).

Compared to the records for Bison and Yellow lakes in Colorado (Anderson, 2011, 2012; Fig. 1), $\delta^{18}O_{carb}$ values of HL are several per mill lower with higher variance for most of the Holocene (Fig. 6). This pattern changes in the late Holocene as carbonate in Bison Lake becomes isotopically lighter than before and approaches the oxygen isotope composition of HL, which maintains a relatively constant mean $\delta^{18}O_{carb}$ value. After approximately 1.5 ka, $\delta^{18}O_{carb}$ variability in HL drops to near the analytical uncertainty (± 0.2‰), while the other records show increased variably (Fig. 6). Despite an increase in summer lake-water $\delta^{18}O$ from −17.8‰ to −10.8‰ today (thick black line, Fig. 2), $\delta^{18}O_{carb}$ values at HL since 1.5 ka only reached a maximum of −16.4‰, and the core-top value is −16.7‰ (Fig. 5). Based on measured lake-water $\delta^{18}O$ and mean water temperatures during the biweekly intervals in which samples were collected from June through October, core-top $\delta^{18}O_{carb}$ at HL should range from −17.4‰ to −10.3‰ based on a standard $\delta^{18}O$ temperature model for estimating $\delta^{18}O_{carb}$ (Leng and Marshall, 2004); using the full range of lake-water temperatures measured through the annual cycle produces a range of −18.3‰ to −8.9‰.

5 Discussion

5.1 Evidence of the 4.2 ka drought in the southern Rocky Mountains

Peak $\delta^{18}O_{carb}$ in HL indicates an abrupt decline in effective moisture or at least a decline in the ratio of snowfall to rain in the Medicine Bow Mountains from approximately 4.2–4 ka (Fig. 5) when evidence from additional climate records shows that aridity affected the southern Rocky Mountains and portions of the Great Plains (Carter et al., 2013; Halfen and Johnson, 2013; Stokes and Gaylord, 1993). The isotope composition of mean annual precipitation potentially became heavier as snowfall declined relative to rain, causing HL's lake-water $\delta^{18}O$ and $\delta^{18}O_{carb}$ to increase. High evaporation could have also amplified these changes. The highest

Table 1. Changes at ca. 4.2 ka inferred from North American climate records near Highway 130 Lake, southeastern Wyoming, USA.

Study	Site name	Region	Climate record	Change at ca. 4.2 ka
Carter et al. (2013, 2017)	Long Lake	Southeastern Wyoming, USA	Fossil pollen	Warming/drying
Halfen et al. (2010)	Casper Dune Field	Southeastern Wyoming, USA	Dune-field chronology	Drying
Stokes and Gaylord (1993)	Ferris/Seminoe Dune Field	Southeastern Wyoming, USA	Dune-field chronology	Drying
Anderson (2011)	Bison Lake	East-central Colorado, USA	Lacustrine carbonate $\delta^{18}O$	No prominent change
Anderson (2012)	Yellow Lake	East-central Colorado, USA	Lacustrine carbonate $\delta^{18}O$	No prominent change
Shuman et al. (2015)	Upper Big Creek Lake	North-central Colorado, USA	Sedimentary lake-level record	Drying
Shuman et al. (2009)	Little Molas Lake	Central Colorado, USA	Sedimentary lake-level record	Drying
Shuman et al. (2014)	Emerald Lake	Central Colorado, USA	Sedimentary lake-level record	Drying

Table 2. Calibrated radiocarbon ages used for the age–depth model.

| Lake	Core	Depth (cm)	Material	Lab number	Age (^{14}C yr BP)	Uncertainty (1σ, ^{14}C yr BP)	Calibrated age ranges (1σ, cal yr BP)		
							Median	Maximum	Minimum
Highway 130 Lake	2A	18	Charcoal	UCIAMS-194167	850	30	748	783	726
		67	Charcoal	UCIAMS-194168	2900	20	3033	3070	2996
	2B	119–121	Charcoal	UCIAMS-194169	2925	15	3073	3144	3004
		154–156	Charcoal	UCIAMS-194170	3660	35	3986	4081	3921
		193–195	Charcoal	UCIAMS-194171	3840	20	4241	4290	4157
		204	Charcoal	UCIAMS-194172	3965	20	4438	4508	4412
		239	Charcoal	UCIAMS-194173	6210	60	7096	7132	7007
		302	Charcoal	UCIAMS-194174	9580	25	10 927	11 074	10 781
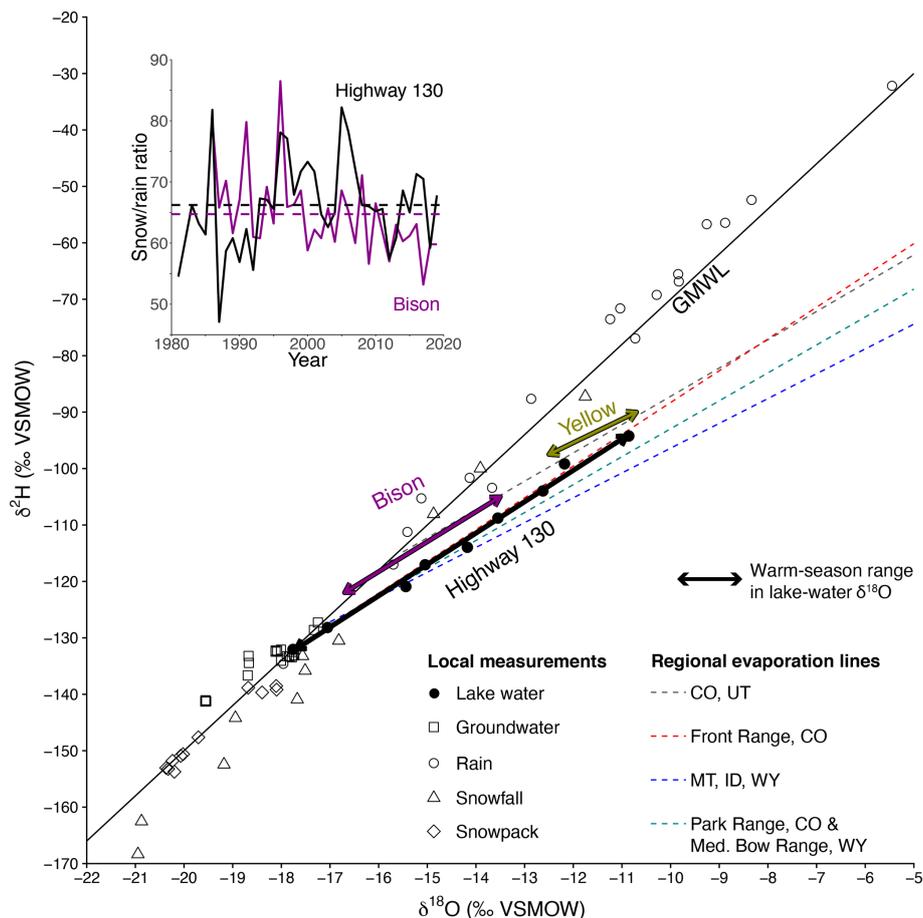
Figure 2. Modern measurements of $\delta^{18}O$ and δD. Samples from the study watershed shown here were collected throughout 2017. Regional evaporation lines (dashed lines; Henderson and Shuman, 2009; Anderson et al., 2016) intersect the global meteoric water line and represent the linear regression of lake-water isotope compositions in a region. Isotopic measurements from the study watershed (open symbols) show the range in isotope compositions of hydrologic inputs to Highway 130 Lake from the watershed. Arrows represent the range in modern $\delta^{18}O$ and δD values of Highway 130 Lake (black), Bison Lake (purple; Anderson, 2011), and Yellow Lake (yellow; Anderson, 2012) throughout the ice-free season, and black dots show the individual measurements at Highway 130 Lake. The inset plot shows the modern annual ratio of snow to rain for the SNOTEL stations nearest Highway 130 Lake (black line) and Bison Lake (purple line), and the dashed lines show the means.

$\delta^{18}O_{carb}$ values at HL coincide with the pollen-inferred precipitation and temperature changes at 4.2 ka at Long Lake, which records 2 centuries of severe drought (Long Lake, Fig. 1; Carter et al., 2013). The excursion also aligns with the long-standing evidence of drought in the Great Plains and southern Rocky Mountains (dune fields, Fig. 1), where a rapid loss of grain-trapping vegetation likely triggered several centuries of increased aeolian transport documented across multiple dune fields (Booth et al., 2005; Forman et al., 2001; Halfen et al., 2010; Stokes and Gaylord, 1993).

Taken together, the records suggest that rapid drying at around 4.2 ka was an important climatic event in the Medicine Bow Mountains even if the drought is not a prominent feature in other paleoclimate studies from the midlatitude Rocky Mountains (Anderson et al., 2008; Brunelle et al., 2013; Feiler et al., 1997; Johnson et al., 2013; Mensing

et al., 2012; Minckley et al., 2012; Shuman et al., 2010; Thompson et al., 1993; Whitlock and Bartlein, 1993), including the nearby $\delta^{18}O_{carb}$ records from Bison and Yellow lakes (Anderson, 2011, 2012). The spatial patterns of late Holocene hydroclimate changes in North America may have been complex compared to other regions, such as the European continent where late Holocene climate variability appears more coherently in climate records (e.g., Deininger et al., 2017). For example, drought status can differ significantly east and west of the Continental Divide, which lies between HL and Bison lakes. Still, the inconsistent evidence complicates interpretations of the 4.2 ka anomaly here and elsewhere (Bradley and Bakke, 2019).

Some paleohydrologic evidence indicates, however, that the event may have been extensive in the southern Rocky Mountains. Sedimentological changes in Little Molas, Emer-
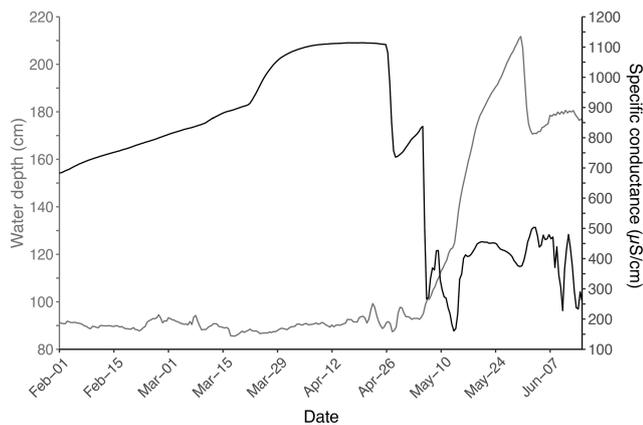
Figure 3. Measurements of water depth (gray line) and specific conductance (black line) at Highway 130 Lake in 2017.

ald, and Upper Big Creek lakes, all high-elevation lakes in Colorado (Fig. 1, Table 1), show substantial hydrological transformation at around 4 ka matching the timing and scale of drought inferred from HL's record (Fig. 7; Shuman et al., 2009a, 2014, 2015). The sediment stratigraphies in these three lakes record low water levels that shifted shoreline sands to the locations of cores collected in 1–5 m water depth today and thus indicate reduced effective moisture at ca. 4.2–4 ka (orange shaded regions, Fig. 7). The median ages of sand layers, indicative of low water at these sites, overlap and fall within the age distribution of the elevated $\delta^{18}O_{carb}$ at HL and overlap with the ages of dune activity in southeastern Wyoming (Halfen and Johnson, 2013; Stokes and Gaylord, 1993); the high-elevation lake locations and geophysical site surveys confirm that the shallow-water sands were not deposited by aeolian activity. Multiple radiocarbon ages also constrain the interval of high carbonate accumulation to approximately 4.4–3 ka, but the sedimentation rate in the interval is sensitive to removal of one of the ages; if the age at ca. 3 ka is out of sequence, it may bias the peak rate of sediment and carbonate accumulation toward high values (but not the timing of the $\delta^{18}O_{carb}$ peak, Figs. 4–7).

The rapid transition from deep-water muds to shallow-water sands as water levels dropped in the Colorado lakes at around 4.2 ka corresponds to changes in pollen assemblages in central Colorado (Jiménez-Moreno et al., 2019) and southeastern Wyoming (Carter et al., 2013), as well as other evidence for drought in North America (Fig. 1, Table 1; Booth et al., 2004). Similar sedimentological features found in lakes along the Atlantic margin from Maine to Pennsylvania date to around 4.2 ka, for example, where the drought appears as one of multiple events linked to circulation changes over the North Atlantic (Li et al., 2007; Marsicek et al., 2013; Newby et al., 2014; Nolan, 2020; Shuman et al., 2019; Shuman and Burrell, 2017). The sequences in the southern Rocky Mountains, however, include uniquely prominent sedimentological

changes from ca. 4.2–4 ka, which align with the single large positive $\delta^{18}O_{carb}$ excursion at HL.

Given the growing evidence of drought within the southern Rocky Mountains at ca. 4.2 ka, a lack of $\delta^{18}O_{carb}$ records of the event in the region, or in North America entirely, is surprising (Anderson et al., 2016; Konecky et al., 2020). However, individual sites respond to a varying mixture of local and regional factors. The stratigraphic evidence of lake-level change in the region is not entirely consistent either and may indicate interactions with different directions of hydroclimate change across seasons, elevations, and latitudes. Stratigraphic features in Hidden Lake, located in northern Colorado just south of Upper Big Creek Lake (Fig. 1) but several hundred meters lower in elevation, document a rapid increase in effective moisture at around 4 ka (Shuman et al., 2009) – the opposite response of the surrounding lakes at higher elevations (Fig. 7). The wet phase was abrupt in onset and termination and lasted from around 4.4–3.7 ka based on multiple radiocarbon ages, and it stands out amid an otherwise gradual trend towards higher water levels since 6 ka (Shuman et al., 2009).

The low-elevation location of Hidden Lake may indicate an important role for increased summer or fall rainfall when high-elevation lake levels declined in response to low winter snowfall. Low winter snow can create favorable surface energy conditions for strong summer convective precipitation (Zhu et al., 2005). The combined effects could have favored the unusually high $\delta^{18}O_{carb}$ at HL by positively shifting the isotope values of mean annual precipitation and HL's water. Alternatively, the reversed hydrologic response of Hidden Lake could indicate antiphased hydroclimate changes in the southern Rocky Mountains between high and low elevations, which is consistent with modern responses to the El Niño–Southern Oscillation (Preece et al., 2021). The active dune fields in east-central Wyoming, however, could confound a simple interpretation of the elevational and seasonally antiphased hydrologic changes, although their activity may depend on soil moisture derived from winter snow (Stokes and Gaylord, 1993). Latitudinal hydroclimate variability could be an additional complicating factor related to the dynamic boundary between the climates of the northern and southern Rocky Mountains (Shinker, 2010; Wise, 2010). The comparison of the radiocarbon age uncertainties of the 4.2 ka paleoshoreline sands at lake-level sites, including Emerald Lake in central Colorado (Figs. 1 and 7), indicates a late Holocene north–south moisture dipole extending across much of the area described here (Shuman et al., 2014).

Given the potential prominence of the 4.2 ka drought at HL and in other southern Rocky Mountain records, it may have been uniquely severe in this region even if it had a complex regional expression at broader spatial scales. The lake-level reconstructions from Colorado contain evidence of other Holocene hydrologic changes (Fig. 7), but the records lack evidence for multiple recurrent, multi-century hydroclimate changes recorded with the 4.2 ka event in places like
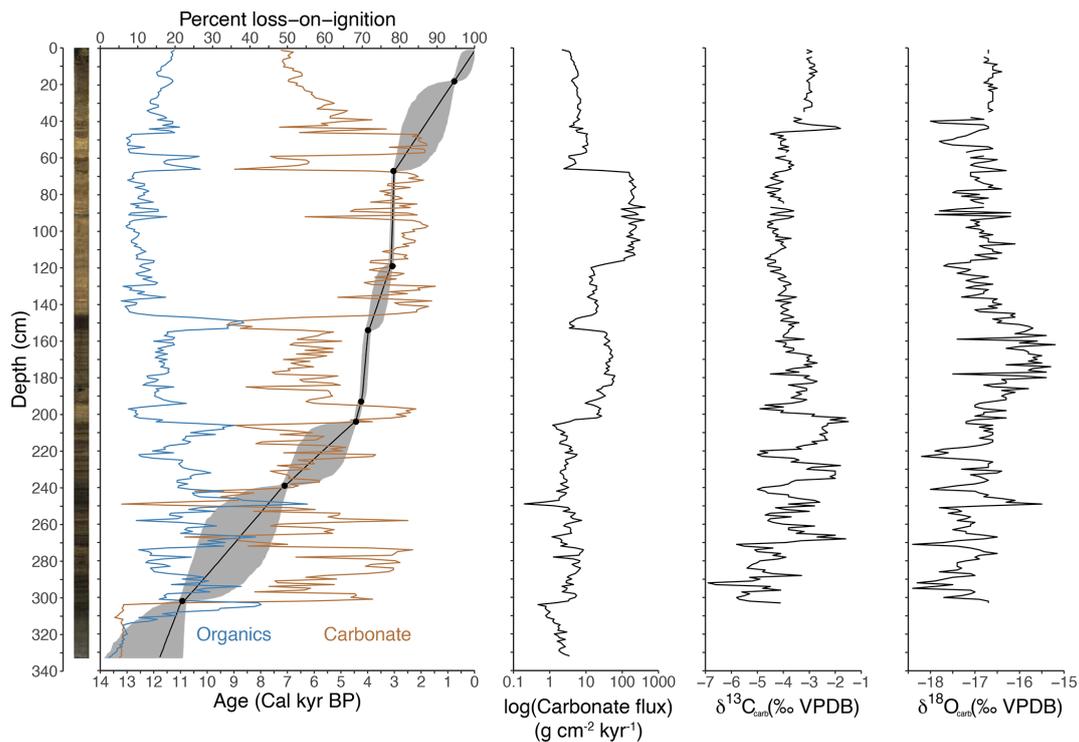
Figure 4. Percent organics, percent carbonate, carbonate flux, $\delta^{13}C_{carb}$, and $\delta^{18}O_{carb}$ are shown by depth alongside an image of the 333 cm long sediment core from Highway 130 Lake. Radiocarbon ages (black dots) were used to create the age–depth model and gray uncertainty band (2σ).

the Atlantic margin (Shuman et al., 2019). Elsewhere, aridity at 4.2 ka may represent just one of several repeated drying events consistent with climate records and simulations from around the world that show drought as a regular feature of late Holocene climate variability (Arz et al., 2006; Bradley and Bakke, 2019; Mayewski et al., 2004; Wanner et al., 2008; Wanner et al., 2015; Yan and Liu, 2019). The midlatitude Rocky Mountain records may suggest that the mid-continent was insulated from some of the abrupt late Holocene climate changes, possibly due to its isolation from the ocean–atmosphere dynamics proposed to play key roles in Holocene variability (Arz et al., 2006; Deininger et al., 2017; Jalali et al., 2019; Yan and Liu, 2019).

5.2   Varying $\delta^{18}O_{carb}$ trends in the southern Rocky Mountains

The marked sensitivity of lake-water $\delta^{18}O$ to hydroclimate changes may make lacustrine carbonates ideal indicators of past droughts like the 4.2 ka event, as documented by $\delta^{18}O_{carb}$ records outside North America (e.g., Bini et al., 2019; Dean et al., 2015) and by our record at HL (Fig. 5), but site-specific hydrologic conditions could complicate the signals. They may generate inconsistent trends among records over both short (seasonal) and long (millennial) timescales (Gibson et al., 2016; Shapley et al., 2008; Steinman and Ab-

bott, 2013; Tyler et al., 2007). Indeed, we observe such inconsistency in the southern Rocky Mountains (Fig. 6).

The hydrologic controls, such as groundwater fluxes and basin morphology, can vary based on a lake's geohydrological setting (Anderson et al., 2016; Dean et al., 2015). Modern lake-water hydrogen and oxygen isotope measurements reveal stronger fractionation by evaporation in HL (thick black line, Fig. 2) compared to Bison and Yellow lakes (purple and yellow lines, Fig. 2; Anderson, 2012), which exhibit a narrower range in modern water isotope compositions and smaller deviation from the global meteoric water line. The differences in hydrologic setting at each lake that produce this pattern are not assumed to override changes in lake-water $\delta^{18}O$ due to climate changes, such as drought. However, the isotopically light carbonate at HL (Fig. 6) is antithetical to the expectation based on evaporatively enriched summer waters (Fig. 2) and suggests that the site may have been sensitive to seasonal dynamics not recorded by Bison or Yellow lakes. The pattern differs from the interpretation that the Bison Lake $\delta^{18}O_{carb}$ was not strongly influenced by evaporation because it was isotopically lighter than other sites like Yellow Lake (Anderson, 2011, 2012). Given the modern water isotope values, we had anticipated that $\delta^{18}O_{carb}$ from HL would be isotopically heavy compared to Bison and Yellow lakes but track similar trends (Anderson, 2012). How-
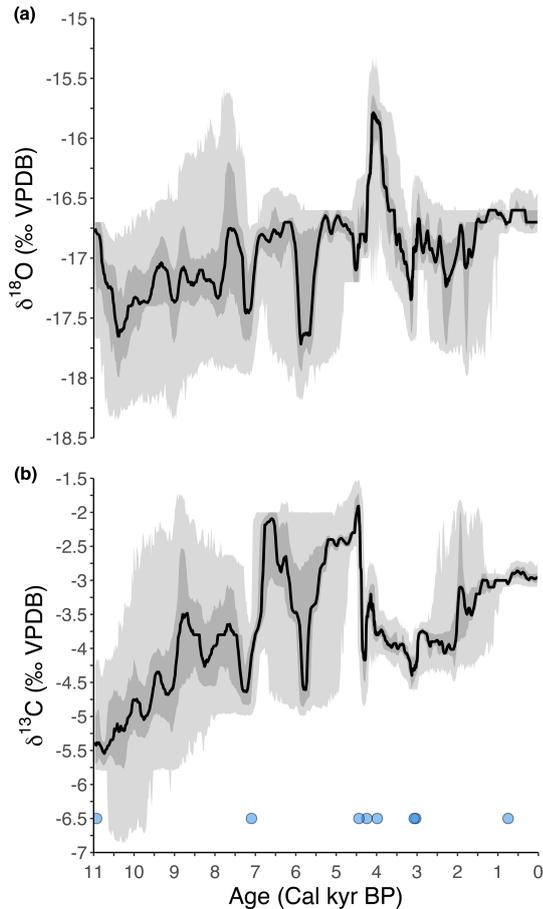
Figure 5. $\delta^{18}O_{carb}$ **(a)** and $\delta^{13}C_{carb}$ **(b)** from Highway 130 Lake. The black line represents the median estimate of the ensemble regression, and the dark and light gray bands show the 50 % and 95 % highest-probability density regions, respectively. The blue dots indicate the calibrated radiocarbon ages used for the age–depth model (refer to Table 2 for calibrated age uncertainties).

Figure 6. $\delta^{18}O_{carb}$ records from **(a)** Yellow Lake (Anderson, 2012), **(b)** Bison Lake (Anderson, 2011), and **(c)** Highway 130 Lake. In panel **(c)** the black line represents the median estimate of the ensemble regression, and the dark and light gray bands show the 50 % and 95 % highest-probability density regions, respectively.

ever, HL lacks the prominent $\delta^{18}O_{carb}$ trend observed at these other sites (Fig. 6).

Differences in the timing of carbonate formation could explain the variability among the records and their sensitivity to the 4.2 ka event. Because rain is isotopically heavier than snow, decreasing snowpack in the watershed should positively shift the isotope composition of HL's water and carbonates. A lower ratio of precipitation to evaporation could also cause a positive shift if carbonates form in evaporated summer waters; however, if the precipitation of carbonates occurs during winter or spring, then $\delta^{18}O_{carb}$ would track the relative contributions of snowfall and rain to its water balance without modification by summer evaporation. Previous studies have shown that the deposition of endogenic carbonate occurs predominantly in the warm summer months when photosynthesis optimizes carbonate production by modifying dissolved CO_2 concentrations and pH (Leng and Marshall, 2004), but the isotopically light carbonate at HL may contra-
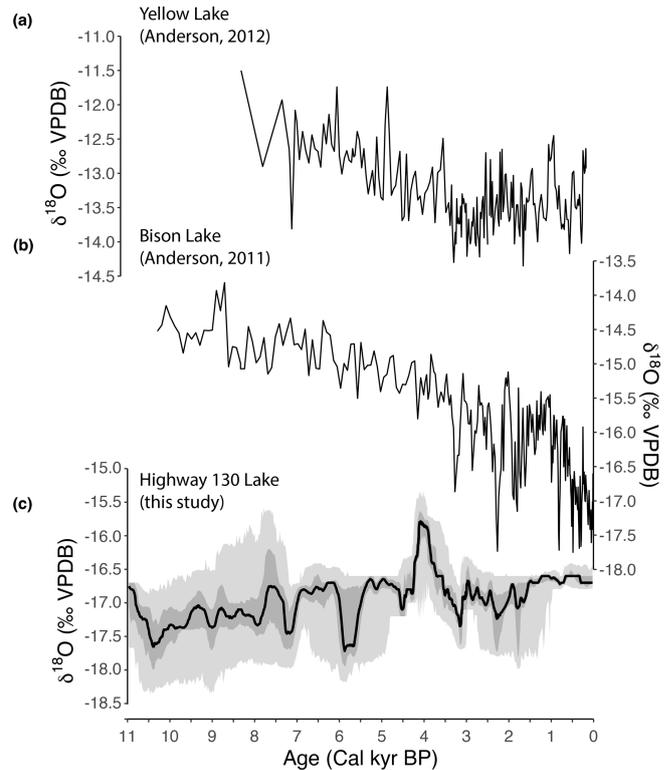
dict this expectation. The observed core-top $\delta^{18}O_{carb}$ value is lower than the calculated fractionation of calcite formation in summer waters, which indicates that HL may not integrate the range of summer lake-water $\delta^{18}O$ today as is assumed for Bison and Yellow lakes (and carbonate lakes in general).

We observe the same pattern in HL's sediment record. $\delta^{18}O_{carb}$ values were below the mean at 6 ka (Fig. 5) when simulated estimates of evaporation rates in the Medicine Bow Mountains were up to 30 % higher than today (Morrill et al., 2019). The enhanced evaporation may explain the more positive mid-Holocene $\delta^{18}O_{carb}$ at Bison and Yellow lakes relative to today (Fig. 6), but if so, such enhanced summer evaporation did not affect $\delta^{18}O_{carb}$ at HL. Because the early springtime deposition of carbonate could capture the isotopic signature of the lake water early in the year, HL may be a better indicator of the snow-to-rain ratio represented by the groundwater inflow into the lake than the seasonal isotopic enrichment of the lake waters by evaporation later in the summer.

The year-round measurements of specific conductance show that conditions favorable for carbonate precipitation may indeed be highest during late winter and spring. In 2017, specific conductance of the water below the surface ice rose from $700\,\mu S\,cm^{-1}$ in early February to $1115\,\mu S\,cm^{-1}$ by
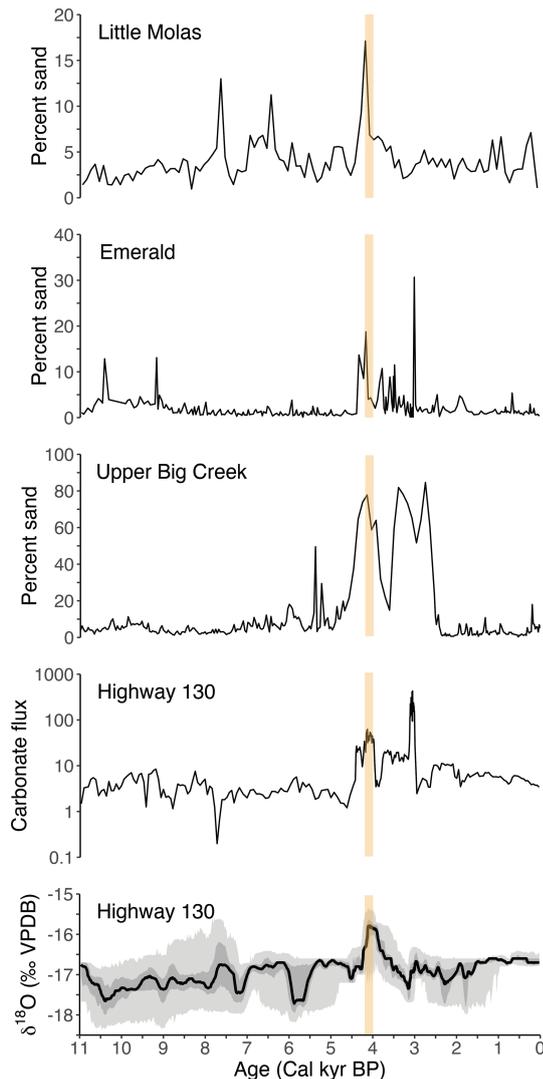
Figure 7. Spikes in the sand content of Little Molas, Emerald, and Upper Big Creek lakes, located in high-elevation watersheds in Colorado (Fig. 1), align with the positive $\delta^{18}O_{carb}$ excursion at Highway 130 Lake and indicate low water from approximately 4.2–4 ka (orange shaded areas) resulting from low effective moisture (Shuman et al., 2009, 2014, 2015).

et al., 2018). If so, ions exsolved from overlying ice raise the conductance of the lake water and pore water within the bottom sediments beyond the concentration in groundwater in winter (Adams and Lasenby, 1985) and create favorable conditions for the rapid deposition of endogenic carbonate in early spring when the isotopic signal would not reflect evaporation or isotopically heavy summer rainfall (open circles, Fig. 2). Spring carbonate formation could also yield a different temperature-dependent effect on the $\delta^{18}O_{carb}$ in HL compared to the other lakes, but the cold spring waters at HL should favor an increase, not decrease, in $\delta^{18}O_{carb}$. Indeed, all of the readily expected process that could complicate a carbonate isotopic record should drive the $\delta^{18}O_{carb}$ in the positive (not negative) direction and underscore the significance of the difference between HL and the other lakes.

As an alternative explanation, the $\delta^{18}O_{carb}$ values could reflect changes in total precipitation rather than seasonality effects because the inflow of Ca-bearing groundwater (which should rise with precipitation) can increase carbonate production and lower $\delta^{18}O_{carb}$ values in alkaline lakes in both ice-free and ice-covered conditions (Shapley et al., 2005), but the weak covariance of weight percent carbonate and $\delta^{18}O_{carb}$ suggests that rates of groundwater inflow did not strongly influence $\delta^{18}O_{carb}$ (Fig. S1a in the Supplement). A weak covariance of $\delta^{13}C_{carb}$ and $\delta^{18}O_{carb}$ indicates short lake-water residence times throughout the lake's history (Fig. S1b; Drummond et al., 1995; Talbot and Kelts, 1990), which could be consistent with rapid flow-through that reduced evaporative enrichment; removing values from 4.2–4 ka only marginally improves the correlation.

A strong negative correlation of weight percent organics and carbonate ($R^2 = -0.79$) suggests that carbonate abundance depends primarily on biological productivity that promoted carbonate dissolution by releasing CO_2 and lowering pH (Fig. S1c; Dean, 1999). Carbonate content from 4.2–4 ka was below the mean despite low organic content (red dots, Fig. S1c) and a high flux of carbonate (Fig. 4), which may represent a shift in HL's water levels and chemistry that favored both acidic conditions and isotopically heavy carbonate (red dots, Fig. S1). Down-core shifts in $\delta^{18}O_{carb}$ produced by seasonal changes in the timing and rate of carbonate formation have been proposed as potential sources of variability within individual records (Fronval et al., 1995; Lamb et al., 2007; Steinman et al., 2012; Steinman and Abbott, 2013; Tyler et al., 2007) and could play a role in the record at HL, but such differences could also generate the variability in the long-term trends observed among records from the southern Rocky Mountains and elsewhere (Bini et al., 2019; Konecky et al., 2020; Roberts et al., 2008).

Many non-climatic factors influence $\delta^{18}O_{carb}$, including carbonate phase and disequilibrium effects, seasonality of precipitation, groundwater fluxes, the isotope compositions of precipitation and groundwater, and local geology. However, such factors are unlikely sources of variability among the regional $\delta^{18}O_{carb}$ records. Down-core carbonate phase

early April, and it remained above $1000 \, \mu S \, cm^{-1}$ throughout April (Fig. 3). These high values would favor carbonate precipitation, whereas the summertime waters are more dilute. Specific conductance of HL and other lakes within the watershed during the summer typically does not exceed $300 \, \mu S \, cm^{-1}$. Melting of lake ice and snowpack rapidly lowers the specific conductance by early May and it remains between $250–300 \, \mu S \, cm^{-1}$ for the remaining ice-free months. The conductance likely remains lower than in winter despite evaporative enrichment of the oxygen isotopes because of groundwater discharge into the lake (Rautio and Korkka-Niemi, 2011), which geophysical surveys, water temperatures, and stable summer water levels at HL support (Liefert

changes are unlikely as only calcite was present in the cores from HL, Bison Lake, and Yellow Lake. We also find no evidence in the sediment core or modern setting at HL to indicate that anthropogenic influence or biologically mediated precipitation of calcite substantially altered $\delta^{18}O_{carb}$ (e.g., carbonate ostracod tests formed in disequilibrium with lake water). Disequilibrium effects associated with biogenic carbonates generally increase $\delta^{18}O_{carb}$ (Holmes and Chivas, 2002; Leng and Marshall, 2004), which would be difficult to reconcile with the surprisingly negative mean and core-top $\delta^{18}O_{carb}$ values at HL based on expectations from the strong enrichment of heavy isotopes by evaporation today and predicted core-top $\delta^{18}O_{carb}$ values.

The seasonal balance of precipitation today is broadly similar among the sites (inset plot, Fig. 2), and the calculated annual precipitation $\delta^{18}O$ value is approximately 1 ‰ lower at HL than at Bison and Yellow lakes (http://waterisotopesDB.org, last access: June 2021). Annual temperature ranges are also similar for the watersheds, making it unlikely that temperature dependence of fractionation could explain the range in $\delta^{18}O_{carb}$ values recorded across the three records unless the different water depths and groundwater influences altered the seasonal temperature progression among lakes. The difference in temperature would need to be large ($\sim 12\,°C$) to explain the offset in $\delta^{18}O_{carb}$ between HL and Bison Lake (and larger for the offset between HL and Yellow Lake), which is unrealistic given the sites' comparable locations and elevations as well as the relatively small temperature changes at midlatitudes since 11 ka (Marsicek et al., 2018). The range in $\delta^{18}O_{carb}$ calculated from the annual range in modern lake-water $\delta^{18}O$ at the lakes does match the observed offsets in the $\delta^{18}O_{carb}$ records of HL, Bison, and Yellow lakes. The timing of carbonate formation thus remains a plausible mechanism for producing the differences. Installing sediment traps during the ice-free season could test the timing of carbonate production.

6 Conclusions

$\delta^{18}O_{carb}$ from HL indicates an abrupt hydroclimate change in the southern Rocky Mountains from approximately 4.2–4 ka that reduced effective moisture or caused less snow to fall than today at high elevations in southern Wyoming. Other $\delta^{18}O_{carb}$ records from the region do not document the drought (Fig. 6; Anderson, 2012), but the event's timing overlaps with evidence of multi-century drought from pollen, lake stratigraphies, and dunes in the southern Rocky Mountains (Carter et al., 2013; Halfen and Johnson, 2013; Shuman et al., 2009, 2014, 2015; Stokes and Gaylord, 1993), the western Great Plains (Booth et al., 2005; Dean, 1997; Halfen and Johnson, 2013; Mason et al., 1997; Stokes and Gaylord, 1993), and elsewhere around the world (Nakamura et al., 2016; Di Rita and Magri, 2019; Scuderi et al., 2019; Xiao et al., 2018).

The timing and magnitude of hydroclimate change in our record agrees with the perspective of a widespread megadrought at around 4.2 ka (Weiss, 2016), but inconsistencies among climate records suggest that (1) site-specific factors can prevent identification of the patterns of abrupt hydroclimate changes, particularly in $\delta^{18}O_{carb}$ records; (2) the hydrologic response in North America and likely elsewhere around the world was spatially complex; and (3) the abrupt hydroclimate changes in the North American mid-continent were more pronounced against background Holocene variability than in many regions such as the Atlantic margin. Consequently, a prolonged "megadrought" at 4.2 ka was likely a significant feature of the hydroclimate history in the midlatitude Rocky Mountains even if that is not true globally.

References

Adams, W. P. and Lasenby, D. C.: The Roles of Snow, Lake Ice and Lake Water in the Distribution of Major Ions in the Ice Cover of a Lake, Ann. Glaciol., 7, 202–207, https://doi.org/10.3189/s0260305500006170, 1985.

Alley, R. B., Mayewski, P. A., Sowers, T., Stuiver, M., Taylor, K. C., and Clark, P. U.: Holocene climatic instability: A prominent, widespread event 8200 yr ago, Geology, 25, 483–486, https://doi.org/10.1130/0091-7613(1997)025<0483:HCIAPW>2.3.CO;2, 1997.

Anderson, L.: Holocene record of precipitation seasonality from lake calcite δ^{18}O in the central Rocky Mountains, United States, Geology, 39, 211–214, https://doi.org/10.1130/G31575.1, 2011.

Anderson, L.: Rocky Mountain hydroclimate: Holocene variability and the role of insolation, ENSO, and the North American Monsoon, Global Planet. Change, 92–93, 198–208, https://doi.org/10.1016/j.gloplacha.2012.05.012, 2012.

Anderson, L., Berkelhammer, M., Barron, J. A., Steinman, B. A., Finney, B. P., and Abbott, M. B.: Lake oxygen isotopes as recorders of North American Rocky Mountain hydroclimate: Holocene patterns and variability at multi-decadal to millennial time scales, Global Planet. Change, 137, 131–148, https://doi.org/10.1016/j.gloplacha.2015.12.021, 2016.

Anderson, R. S., Allen, C. D., Toney, J. L., Jass, R. B., and Bair, A. N.: Holocene vegetation and fire regimes in subalpine and mixed conifer forests, southern Rocky Mountains, USA, Int. J. Wildland Fire, 17, 96–114, https://doi.org/10.1071/WF07028, 2008.

Arz, H. W., Lamy, F., and Pätzold, J.: A pronounced dry event recorded around 4.2 ka in brine sediments from the northern Red Sea, Quaternary Res., 66, 432–441, https://doi.org/10.1016/j.yqres.2006.05.006, 2006.

Ault, T. R., George, S. S., Smerdon, J. E., Coats, S., Mankin, J. S., Carrillo, C. M., Cook, B. I., and Stevensong, S.: A robust null hypothesis for the potential causes of megadrought in Western North America, J. Climate, 31, 3–24, https://doi.org/10.1175/JCLI-D-17-0154.1, 2018.

Bello, R. and Smith, J. D.: The Effect of Weather Variability on the Energy Balance of a Lake in the Hudson Bay Lowlands, Canada, INSTAAR, Univ. Color., 22, 98–107, 1990.

Bini, M., Zanchetta, G., Perşoiu, A., Cartier, R., Català, A., Cacho, I., Dean, J. R., Di Rita, F., Drysdale, R. N., Finnè, M., Isola, I., Jalali, B., Lirer, F., Magri, D., Masi, A., Marks, L., Mercuri, A. M., Peyron, O., Sadori, L., Sicre, M.-A., Welc, F., Zielhofer, C., and Brisset, E.: The 4.2 ka BP Event in the Mediterranean region: an overview, Clim. Past, 15, 555–577, https://doi.org/10.5194/cp-15-555-2019, 2019.

Booth, R. K., Jackson, S. T., Forman, S. L., Kutzbach, J. E., Bettis, E. A., Kreig, J., and Wright, D. K.: A severe centennial-scale drought in mid-continental North America 4200 years ago and apparent global linkages, Holocene, 15, 321–328, https://doi.org/10.1191/0959683605hl825ft, 2005.

Bradley, R. S. and Bakke, J.: Is there evidence for a 4.2 ka BP event in the northern North Atlantic region?, Clim. Past, 15, 1665–1676, https://doi.org/10.5194/cp-15-1665-2019, 2019.

Brunelle, A., Minckley, T. A., Lips, E., and Burnett, P.: A record of Lateglacial/Holocene environmental change from a high-elevation site in the Intermountain West, USA, J. Quaternary Sci., 28, 103–112, https://doi.org/10.1002/jqs.2600, 2013.

Carter, V. A., Brunelle, A., Minckley, T. A., Dennison, P. E., and Power, M. J.: Regionalization of fire regimes in the Central Rocky Mountains, USA, Quaternary Res., 80, 406–416, https://doi.org/10.1016/j.yqres.2013.07.009, 2013.

Carter, V. A., Brunelle, A., Minckley, T. A., Shaw, J. D., DeRose, R. J., and Brewer, S.: Climate variability and fire effects on quaking aspen in the central Rocky Mountains, USA, J. Biogeogr., 44, 1280–1293, https://doi.org/10.1111/jbi.12932, 2017.

Carter, V. A., Shinker, J. J., and Preece, J.: Drought and vegetation change in the central Rocky Mountains and western Great Plains: potential climatic mechanisms associated with megadrought conditions at 4200 cal yr BP, Clim. Past, 14, 1195–1212, https://doi.org/10.5194/cp-14-1195-2018, 2018.

Clark, P. U., Webb, R. S., and Keigwin, L. D.: Mechanisms of global climate change at millennial time scales, American Geophysical Union, Washington, DC, ISBN 978-1-118-66474-2, https://doi.org/10.1029/GM112, 1999.

Dean, J. R., Jones, M. D., Leng, M. J., Noble, S. R., Metcalfe, S. E., Sloane, H. J., Sahy, D., Eastwood, W. J., and Roberts, C. N.: Eastern Mediterranean hydroclimate over the late glacial and Holocene, reconstructed from the sediments of Nar lake, central Turkey, using stable isotopes and carbonate mineralogy, Quaternary Sci. Rev., 124, 162–174, https://doi.org/10.1016/j.quascirev.2015.07.023, 2015.

Dean, W. E.: Rates, timing, and cyclicity of Holocene eolian activity in north-central United States: Evidence from varved lake sediments, Geology, 25, 331–334, https://doi.org/10.1130/0091-7613(1997)025<0331:RTACOH>2.3.CO;2, 1997.

Dean, W. E.: The carbon cycle and biogeochemical dynamics in lake sediments, J. Paleolimnol., 21, 375–393, https://doi.org/10.1023/A:1008066118210, 1999.

Deininger, M., McDermott, F., Mudelsee, M., Werner, M., Frank, N., and Mangini, A.: Coherency of late Holocene European speleothem δ^{18}O records linked to North Atlantic Ocean circulation, Clim. Dynam., 49, 595–618, https://doi.org/10.1007/s00382-016-3360-8, 2017.

Denniston, R. F., Gonzalez, L. A., Baker, R. G., Asmerom, Y., Reagan, M. K., Edwards, R. L., and Alexander, E. C.: Speleothem evidence for Holocene fluctuations of the prairie-forest ecotone, Holocene 6, 671–676, 1992

Di Rita, F. and Magri, D.: The 4.2 ka event in the vegetation record of the central Mediterranean, Clim. Past, 15, 237–251, https://doi.org/10.5194/cp-15-237-2019, 2019.

Drummond, C. N., Patterson, W. P., and Walker, J. C. G.: Climatic forcing of carbon-oxygen isotopic covariance in temperate-region marl lakes, Geology, 23, 1031–1034, https://doi.org/10.1130/0091-7613(1995)023<1031:cfocoi>2.3.co;2, 1995.

Feiler, E. J., Scott, R., and Koehler, A.: Late Quaternary Paleoenvironments of the White River Plateau, Colorado, U.S.A., Arctic Alpine Res., 29, 53–62, http://www.jstor.org/stable/1551836 (last access: June 2021), 1997.

Forman, S. L., Oglesby, R., and Webb, R. S.: Temporal and spatial patterns of Holocene dune activity on the Great Plains of North America: Megadroughts and climate links, Glob. Planet. Change, 29, 1–29, https://doi.org/10.1016/S0921-8181(00)00092-8, 2001.

Fronval, T., Jensen, N. B., and Buchardt, B.: Oxygen isotope disequilibrium precipitation of calcite in Lake Arreso,

Denmark, Geology, 23, 463–466, https://doi.org/10.1130/0091-7613(1995)023<0463:OIDPOC>2.3.CO;2, 1995.

Gibson, J. J., Birks, S. J., Yi, Y., Moncur, M. C., and McEachern, P. M.: Stable isotope mass balance of fifty lakes in central Alberta: Assessing the role of water balance parameters in determining trophic status and lake level, J. Hydrol. Reg. Stud., 6, 13–25, https://doi.org/10.1016/j.ejrh.2016.01.034, 2016.

Halfen, A. F. and Johnson, W. C.: A review of Great Plains dune field chronologies, Aeolian Res., 10, 135–160, https://doi.org/10.1016/j.aeolia.2013.03.001, 2013.

Halfen, A. F., Fredlund, G. G., and Mahan, S. A.: Holocene stratigraphy and chronology of the Casper Dune Field, Casper, Wyoming, USA, Holocene, 20, 773–783, https://doi.org/10.1177/0959683610362812, 2010.

Henderson, A. K. and Shuman, B. N.: Hydrogen and oxygen isotopic compositions of lake water in the western United States, Geol. Soc. Am. Bull., 121, 1179–1189, https://doi.org/10.1130/B26441.1, 2009.

Holmes, J. A. and Chivas, A. R.: Ostracod shell chemistry – overview, Geophys. Un. Geophys. Monogr. Ser., 131, 185–204, 2002.

Houston, R. S. and Karlstrom, K. E.: Geologic map of Precambrian metasedimentary rocks of the Medicine Bow Mountains, Albany and Carbon counties, Wyoming, U.S. Geol. Surv. Misc. Investig. Map, I-2280. Sc, https://doi.org/10.3133/i2280, 1992.

Huang, C. C., Pang, J., Zha, X., Su, H., and Jia, Y.: Extraordinary floods related to the climatic event at 4200 a BP on the Qishuihe River, middle reaches of the Yellow River, China, Quaternary Sci. Rev., 30, 460–468, https://doi.org/10.1016/j.quascirev.2010.12.007, 2011.

Jalali, B., Sicre, M.-A., Azuara, J., Pellichero, V., and Combourieu-Nebout, N.: Influence of the North Atlantic subpolar gyre circulation on the 4.2 ka BP event, Clim. Past, 15, 701–711, https://doi.org/10.5194/cp-15-701-2019, 2019.

Jiménez-Moreno, G., Anderson, R. S., Shuman, B. N., and Yackulic, E.: Forest and lake dynamics in response to temperature, North American monsoon and ENSO variability during the Holocene in Colorado (USA), Quaternary Sci. Rev., 211, 59–72, https://doi.org/10.1016/j.quascirev.2019.03.013, 2019.

Johnson, B. G., Jiménez-Moreno, G., Eppes, M. C., Diemer, J. A., and Stone, J. R.: A multiproxy record of postglacial climate variability from a shallowing, 12-m deep sub-alpine bog in the southeastern San Juan Mountains of Colorado, USA, Holocene, 23, 1028–1038, https://doi.org/10.1177/0959683613479682, 2013.

Kahle, D. and Wickham, H.: ggmap: Spatial Visualization with ggplot2, R J., 5, 144–161, 2013.

Konecky, B. L., McKay, N. P., Churakova (Sidorova), O. V., Comas-Bru, L., Dassié, E. P., DeLong, K. L., Falster, G. M., Fischer, M. J., Jones, M. D., Jonkers, L., Kaufman, D. S., Leduc, G., Managave, S. R., Martrat, B., Opel, T., Orsi, A. J., Partin, J. W., Sayani, H. R., Thomas, E. K., Thompson, D. M., Tyler, J. J., Abram, N. J., Atwood, A. R., Cartapanis, O., Conroy, J. L., Curran, M. A., Dee, S. G., Deininger, M., Divine, D. V., Kern, Z., Porter, T. J., Stevenson, S. L., von Gunten, L., and Iso2k Project Members: The Iso2k database: a global compilation of paleo-δ^{18}O and δ^2H records to aid understanding of Common Era climate, Earth Syst. Sci. Data, 12, 2261–2288, https://doi.org/10.5194/essd-12-2261-2020, 2020.

Lamb, H. F., Leng, M. J., Telford, R. J., Ayenew, T., and Umer, M.: Oxygen and carbon isotope composition of authigenic carbonate from an Ethiopian lake: A climate record of the last 2000 years, Holocene, 17, 517–526, https://doi.org/10.1177/0959683607076452, 2007.

Leng, M. J. and Marshall, J. D.: Palaeoclimate interpretation of stable isotope data from lake sediment archives, Quaternary Sci. Rev., 23, 811–831, https://doi.org/10.1016/j.quascirev.2003.06.012, 2004.

Li, Y. X., Yu, Z., and Kodama, K. P.: Sensitive moisture response to Holocene millennial-scale climate variations in the Mid-Atlantic region, USA, Holocene, 17, 3–8, https://doi.org/10.1177/0959683606069386, 2007.

Liefert, D. T. and Shuman, B. N.: Highway 130 Lake, Wyoming 11,700 Year Stable Isotope and Carbonate Data, NOAA [data set], https://doi.org/10.25921/dtev-ht06, 2022.

Liefert, D. T., Shuman, B. N., Parsekian, A. D., and Mercer, J. J.: Why Are Some Rocky Mountain Lakes Ephemeral?, Water Resour. Res., 54, 5245–5263, https://doi.org/10.1029/2017WR022261, 2018.

Marsicek, J., Shuman, B. N., Bartlein, P. J., Shafer, S. L., and Brewer, S.: Reconciling divergent trends and millennial variations in Holocene temperatures, Nature, 554, 92–96, https://doi.org/10.1038/nature25464, 2018.

Marsicek, J. P., Shuman, B., Brewer, S., Foster, D. R., and Oswald, W. W.: Moisture and temperature changes associated with the mid-Holocene Tsuga decline in the northeastern United States, Quaternary Sci. Rev., 80, 129–142, https://doi.org/10.1016/j.quascirev.2013.09.001, 2013.

Mason, J. P., Swinehart, J. B., and Loope, D. B.: Holocene history of lacustrine and marsh sediments in a dune blocked drainage, Southwestern Nebraska Sand Hills, U.S.A., J. Paleolimnol., 17, 67–83, https://doi.org/10.1023/A:1007917110965, 1997.

Mayewski, P. A., Rohling, E. E., Stager, J. C., Karlén, W., Maasch, K. A., Meeker, L. D., Meyerson, E. A., Gasse, F., van Kreveld, S., Holmgren, K., Lee-Thorp, J., Rosqvist, G., Rack, F., Staubwasser, M., Schneider, R. R., and Steig, E. J.: Holocene climate variability, Quaternary Res., 62, 243–255, https://doi.org/10.1016/j.yqres.2004.07.001, 2004.

McKay, N. P., Emile-Geay, J., and Khider, D.: geoChronR – an R package to model, analyze, and visualize age-uncertain data, Geochronology, 3, 149–169, https://doi.org/10.5194/gchron-3-149-2021, 2021.

Mensing, S., Korfmacher, J., Minckley, T., and Musselman, R.: A 15,000 year record of vegetation and climate change from a treeline lake in the Rocky Mountains, Wyoming, USA, Holocene, 22, 739–748, https://doi.org/10.1177/0959683611430339, 2012.

Minckley, T. A., Shriver, R. K., and Shuman, B.: Resilience and regime change in a southern Rocky Mountain ecosystem during the past 17 000 years TL, Ecol. Monogr., 82, 49–68, https://doi.org/10.1890/11-0283.1, 2012.

Mock, C.: Climate controls and spatial variations of precipitation in the western United States, J. Climate, 9, 1111–1125, 1996.

Morrill, C., Meador, E., Livneh, B., Liefert, D. T., and Shuman, B. N.: Quantitative model-data comparison of mid Holocene lake-level change in the central Rocky Mountains, Clim. Dynam., 53, 1077–1094, https://doi.org/10.1007/s00382-019-04633-3, 2019.

Musselman, R. C., Connell, B. H., Conrad, M. A., Dufford, R. G., Fox, D. G., Haines, J. D., Hasfurther, V. C., Hopper, R. W. E.,

Humphries, H. C., Kerr, G. L., Kondratieff, B. C., Parks, G., Regan, C. M., Rochette, E. A., Schoettle, A. W., Simmons, C. L., Sommerfeld, R. A., Vertucci, F. A., Walthall, P. M., Wetstein, J., Wooldridge, G. L., and Zeller, K. F.: The Glacier Lakes Ecosystem Experiments Site, US Department of Agriculture, Forest Service, https://doi.org/10.2737/RM-GTR-249, 1992.

Nakamura, A., Yokoyama, Y., Maemoku, H., Yagi, H., Okamura, M., Matsuoka, H., Miyake, N., Osada, T., Adhikari, D. P., Dangol, V., Ikehara, M., Miyairi, Y., and Matsuzaki, H.: Weak monsoon event at 4.2 ka recorded in sediment from Lake Rara, Himalayas, Quaternary Int., 397, 349–359, https://doi.org/10.1016/j.quaint.2015.05.053, 2016.

Newby, P. E., Shuman, B. N., Donnelly, J. P., Karnauskas, K. B., and Marsicek, J.: Centennial-to-millennial hydrologic trends and variability along the North Atlantic Coast, USA, during the Holocene, Geophys. Res. Lett., 41, 4300–4307, https://doi.org/10.1002/2014GL060183, 2014.

Nolan, C.: Using Co-Located Lake and Bog Records to Improve Inferences on Late Quaternary Climate and Ecology, University of Arizona, https://repository.arizona.edu/handle/10150/633144 (last access: June 2021), 2020.

Parnell, A. C., Haslett, J., Allen, J. R. M., Buck, C. E., and Huntley, B.: A flexible approach to assessing synchroneity of past events using Bayesian reconstructions of sedimentation history, Quaternary Sci. Rev., 27, 1872–1885, https://doi.org/10.1016/j.quascirev.2008.07.009, 2008.

Preece, J. R., Shinker, J. J., Riebe, C. S., and Minckley, T. A.: Elevation-dependent precipitation response to El Niño-Southern oscillation revealed in headwater basins of the US central Rocky Mountains, Int. J. Climatol., 21, 1199–1210, https://doi.org/10.1002/joc.6790, 2021.

Railsback, L. B., Liang, F., Brook, G. A., Voarintsoa, N. R. G., Sletten, H. R., Marais, E., Hardt, B., Cheng, H., and Edwards, R. L.: The timing, two-pulsed nature, and variable climatic expression of the 4.2 ka event: A review and new high-resolution stalagmite data from Namibia, Quaternary Sci. Rev., 186, 78–90, https://doi.org/10.1016/j.quascirev.2018.02.015, 2018.

Ran, M. and Chen, L.: The 4.2 ka BP climatic event and its cultural responses, Quaternary Int., 521, 158–167, https://doi.org/10.1016/j.quaint.2019.05.030, 2019.

Rautio, A. and Korkka-Niemi, K.: Characterization of groundwater-lake water interactions at Pyhäjärvi, a lake in SW Finland, Boreal Environ. Res., 16, 363–380, 2011.

Reimer, P. J., Bard, E., Bayliss, A., Beck, J. W., Blackwell, P. G., Ramsey, C. B., Buck, C.E., Cheng, H., Edwards, R. L., Friedrich, M., and Grootes, P. M.: IntCal13 and Marine13 radiocarbon age calibration curves 0–50,000 years cal BP, Radiocarbon, 55, 1869–1887, https://doi.org/10.2458/azu_js_rc.55.16947, 2013.

Renssen, H., Goosse, H., and Muscheler, R.: Coupled climate model simulation of Holocene cooling events: oceanic feedback amplifies solar forcing, Clim. Past, 2, 79–90, https://doi.org/10.5194/cp-2-79-2006, 2006.

Roberts, N., Jones, M. D., Benkaddour, A., Eastwood, W. J., Filippi, M. L., Frogley, M. R., Lamb, H. F., Leng, M. J., Reed, J. M., Stein, M., Stevens, L., Valero-Garcés, B., and Zanchetta, G.: Stable isotope records of Late Quaternary climate and hydrology from Mediterranean lakes: the ISOMED synthesis, Quaternary Sci. Rev., 27, 2426–2441, https://doi.org/10.1016/j.quascirev.2008.09.005, 2008.

Roland, T. P., Caseldine, C. J., Charman, D. J., Turney, C. S. M., and Amesbury, M. J.: Was there a "4.2 ka event" in Great Britain and Ireland? Evidence from the peatland record, Quaternary Sci. Rev., 83, 11–27, https://doi.org/10.1016/j.quascirev.2013.10.024, 2014.

Rosenberry, D. O. and LaBaugh, J. W.: Field Techniques for Estimating Water Fluxes Between Surface Water and Ground Water, Report, Geological Survey (U.S.), https://doi.org/10.3133/tm4D2, 2008.

Scuderi, L. A., Yang, X., Ascoli, S. E., and Li, H.: The 4.2 ka BP Event in northeastern China: a geospatial perspective, Clim. Past, 15, 367–375, https://doi.org/10.5194/cp-15-367-2019, 2019.

Shapley, M. D., Ito, E., and Donovan, J. J.: Authigenic calcium carbonate flux in groundwater-controlled lakes: Implications for lacustrine paleoclimate records, Geochim. Cosmochim. Ac., 69, 2517–2533, https://doi.org/10.1016/j.gca.2004.12.001, 2005.

Shapley, M. D., Ito, E., and Donovan, J. J.: Isotopic evolution and climate paleorecords: Modeling boundary effects in groundwater-dominated lakes, J. Paleolimnol., 39, 17–33, https://doi.org/10.1007/s10933-007-9092-3, 2008.

Shinker, J. J.: Visualizing spatial heterogeneity of western U.S. climate variability, Earth Interact., 14, 1–15, https://doi.org/10.1175/2010EI323.1, 2010.

Shuman, B., Henderson, A. K., Colman, S. M., Stone, J. R., Fritz, S. C., Stevens, L. R., Power, M. J., and Whitlock, C.: Holocene lake-level trends in the Rocky Mountains, U.S.A., Quaternary Sci. Rev., 28, 1861–1879, https://doi.org/10.1016/j.quascirev.2009.03.003, 2009.

Shuman, B., Pribyl, P., Minckley, T. A., and Shinker, J. J.: Rapid hydrologic shifts and prolonged droughts in Rocky Mountain headwaters during the Holocene, Geophys. Res. Lett., 37, L06701, https://doi.org/10.1029/2009GL042196, 2010.

Shuman, B. N. and Burrell, S. A.: Centennial to millennial hydroclimatic fluctuations in the humid northeast United States during the Holocene, Quaternary Res., 88, 514–524, https://doi.org/10.1017/qua.2017.62, 2017.

Shuman, B. N. and Serravezza, M.: Patterns of hydroclimatic change in the Rocky Mountains and surrounding regions since the last glacial maximum, Quaternary Sci. Rev., 173, 58–77, https://doi.org/10.1016/j.quascirev.2017.08.012, 2017.

Shuman, B. N., Carter, G. E., Hougardy, D. D., Powers, K., and Shinker, J. J.: A north-south moisture dipole at multi-century scales in the Central and Southern Rocky Mountains, U.S.A., during the late Holocene, Rocky Mt. Geol., 49, 33–49, https://doi.org/10.2113/gsrocky.49.1.33, 2014.

Shuman, B. N., Pribyl, P., and Buettner, J.: Hydrologic changes in Colorado during the mid-Holocene and Younger Dryas, Quaternary Res., 84, 187–199, https://doi.org/10.1016/j.yqres.2015.07.004, 2015.

Shuman, B. N., Marsicek, J., Oswald, W. W., and Foster, D. R.: Predictable hydrological and ecological responses to Holocene North Atlantic variability, P. Natl. Acad. Sci. USA, 116, 5985–5990, https://doi.org/10.1073/pnas.1814307116, 2019.

Steinman, B. A. and Abbott, M. B.: Isotopic and hydrologic responses of small, closed lakes to climate variability: Hydroclimate reconstructions from lake sediment oxygen isotope records and mass balance models, Geochim. Cosmochim. Ac., 105, 342–359, https://doi.org/10.1016/j.gca.2012.11.027, 2013.

Steinman, B. A., Abbott, M. B., Nelson, D. B., Stansell, N. D., Finney, B. P., Bain, D. J., and Rosenmeier, M. F.: Isotopic and hydrologic responses of small, closed lakes to climate variability: Comparison of measured and modeled lake level and sediment core oxygen isotope records, Geochim. Cosmochim. Ac., 105, 455–471, https://doi.org/10.1016/j.gca.2012.11.026, 2012.

Stewart, R. B. and Rouse, W. R.: A Simple Method for Determining the Evaporation From Shallow Lakes and Ponds, Water Resour. Res., 12, 623–628, https://doi.org/10.1029/WR012i004p00623, 1976.

Stokes, S. and Gaylord, D. R.: Optical Dating of Holocene Dune Sands in the Ferris Dune Field, Wyoming, Quaternary Res., 39, 274–281, 1993.

Talbot, M. R.: A review of the palaeohydrological interpretation of carbon and oxygen isotpic rations in pimary lacustrine carbonates, Chem. Geol., 80, 261–279, 1990.

Talbot, M. R. and Kelts, K.: Paleolimnological signatures from carbon and oxygen isotopic ratios in carbonates from organic-rich lacustrine sediments, Lacustrine Explor. Case Stud. Mod. Analog., 50, 99–112, https://doi.org/10.1306/M50523C6, 1990.

Tan, L. C., An, Z. S., Cai, Y. J., and Long, H.: Hydrological representation of the 4.2 ka BP event in China and its global linkages, Geol. Rev., 54, 94–104, 2008.

Thompson, R. S., Whitlock, C., Bartlein, P. J., Harrison, S. P., and Geoffrey Spaulding, W.: Climatic Changes in the Western United States since 18,000 yr B.P., in: Global Climates since the Last Glacial Maximum, edited by: Wright Jr., H. E., Kutzbach, J. E., Webb III, T., Ruddiman, W. F., Street-Perrott, F. A., and Bartlein, P. J., University of Minnesota Press, 468–513, 1993.

Tyler, J. J., Leng, M. J., and Arrowsmith, C.: Seasonality and the isotope hydrology of Lochnagar, a Scottish mountain lake: Implications for palaeoclimate research, Holocene, 17, 717–727, https://doi.org/10.1177/0959683607080513, 2007.

Von Grafenstein, U., Erlenkeuser, H., Müller, J., Jouzel, J., and Johnsen, S.: The cold event 8200 years ago documented in oxygen isotope records of precipitation in Europe and Greenland, Clim. Dynam., 14, 73–81, https://doi.org/10.1007/s003820050210, 1998.

Walker, M., Gibbard, P., Head, M. J., Berkelhammer, M., Björck, S., Cheng, H., Cwynar, L. C., Fisher, D., Gkinis, V., Long, A., Lowe, J., Newnham, R., Rasmussen, S. O., and Weiss, H.: Formal Subdivision of the Holocene Series/Epoch: A Summary, J. Geol. Soc. India, 93, 135–141, https://doi.org/10.1007/s12594-019-1141-9, 2019.

Wang, Y., Cheng, H., Edwards, R. L., He, Y., Kong, X., An, Z., Wu, J., Kelly, M. J., Dykoski, C. A., and Li, X.: The Holocene Asian monsoon: links to solar changes and North Atlantic climate, Science, 308, 854–857, https://doi.org/10.1126/science.1106296, 2005.

Wanner, H., Beer, J., Bütikofer, J., Crowley, T. J., Cubasch, U., Flückiger, J., Goosse, H., Grosjean, M., Joos, F., Kaplan, J. O., Küttel, M., Müller, S. A., Prentice, I. C., Solomina, O., Stocker, T. F., Tarasov, P., Wagner, M., and Widmann, M.: Mid- to Late Holocene climate change: an overview, Quaternary Sci. Rev., 27, 1791–1828, https://doi.org/10.1016/j.quascirev.2008.06.013, 2008.

Wanner, H., Solomina, O., Grosjean, M., Ritz, S. P., and Jetel, M.: Structure and origin of Holocene cold events, Quaternary Sci. Rev., 30, 3109–3123, https://doi.org/10.1016/j.quascirev.2011.07.010, 2011.

Wanner, H., Wanner, H., Mercolli, L., Mercolli, L., Grosjean, M., Grosjean, M., and Ritz, S. P.: Holocene climate variability and change; a data-based review, J. Geol. Soc. Lond., 172, 254–263, https://doi.org/10.1144/jgs2013-101, 2015.

Weiss, H.: Climate change and cultural evolution across the world, Past Glob. Chang. Mag., 24, 62–63, https://doi.org/10.22498/pages.24.2.55, 2016.

Weiss, H.: Interactive comment on "Is there evidence for a 4.2 ka BP event in the northern North Atlantic region?" by R. Bradley and J. Bakke, Clim. Past, https://doi.org/10.5194/cp-2018-162-RC2, 2019.

Whitlock, C. and Bartlein, P. J.: Spatial Variations of Holocene Climatic Change in the Yellowstone Region, Quaternary Res., 39, 231–238, 1993.

Wise, E. K.: Spatiotemporal variability of the precipitation dipole transition zone in the western United States, Geophys. Res. Lett., 37, L07706, https://doi.org/10.1029/2009gl042193, 2010.

Xiao, J., Zhang, S., Fan, J., Wen, R., Zhai, D., Tian, Z., and Jiang, D.: The 4.2 ka BP event: multi-proxy records from a closed lake in the northern margin of the East Asian summer monsoon, Clim. Past, 14, 1417–1425, https://doi.org/10.5194/cp-14-1417-2018, 2018.

Yan, M. and Liu, J.: Physical processes of cooling and megadrought during the 4.2 ka BP event: results from TraCE-21ka simulations, Clim. Past, 15, 265–277, https://doi.org/10.5194/cp-15-265-2019, 2019.

Zhang, H., Cheng, H., Cai, Y., Spötl, C., Kathayat, G., Sinha, A., Edwards, R. L., and Tan, L.: Hydroclimatic variations in southeastern China during the 4.2 ka event reflected by stalagmite records, Clim. Past, 14, 1805–1817, https://doi.org/10.5194/cp-14-1805-2018, 2018.

Zhu, C., Lettenmaier, D. P., and Cavazos, T.: Role of antecedent land surface conditions on North American monsoon rainfall variability, J. Climate, 18, 3104–3121, https://doi.org/10.1175/JCLI3387.1, 2005.